



Microstructure and corrosion properties of Al(Ni/TiB₂) intermetallic matrix composite coatings

by A.P.I. Popoola*, S.L. Pityana†, and O.M. Popoola*

Synopsis

Laser coatings are used for a wide variety of applications. TiB₂/Ni intermetallic matrix composite coatings were fabricated on Al-substrate by a high power Rofin Sinar Nd: YAG solid-state laser. The characterization of the coatings was carried out by optical microscopy (OM), scanning electron microscopy (SEM/EDS) and X-ray Diffraction (XRD). Electrochemical study of the laser coatings in 3.65 per cent NaCl at room temperature revealed that with very high weight proportion of nickel the corrosion resistance of the coatings deteriorated due the presence of AlB₁₀ phase. 50 wt per cent TiB₂+50 wt per cent Ni laser coatings exhibited the highest corrosion resistance in test solution.

Keywords

Corrosion, protective film, laser surface alloying, reinforcement.

Introduction

Enormous research efforts have been directed towards the fabrication of surface coatings, which are formed by exothermic reactions between reinforcements and substrates. Thermodynamically stable composites/intermetallics coatings can be formed on the surface of metals and alloys by laser surface alloying process (LSA). LSA is an advanced materials processing method that offers numerous advantages over alternative methods: good metallurgical bonds between the reinforcement materials and the substrates, minimized crack and pore formation and achievement of improved mechanical and chemical properties. For these reasons, LSA has become a versatile process for tailoring the surface properties of components and alloys. This involves low heat input at the surface of the substrate that results in localized melting; with the simultaneous injection of alloying powder the formation of new alloy layer is accomplished. The heat input is a thermodynamic property that is a function of temperature and the laser alloying speed. LSA can produce surface layers with distinct microstructures and non-equilibrium compositions. The degree of enhancement

depends on the final microstructure formed, which in turn depends on the composition and properties of the materials alloyed and on the laser processing parameters used¹⁻³.

Corrosion is one of the most frequently encountered causes of failure for components. Corrosion is a complex series of oxidation/reduction reactions between the metal/alloy surfaces and liquid media. Nearly all metals will corrode to some degree. The rate and the extent of the corrosion depends on the degree of dissimilarity of the metals/alloys and the physical and chemical characteristics of the media, metal/alloy and the environment. Such metal/alloy and environment is aluminium and chloride respectively. The surfaces of Al and its alloys are subject to corrosion especially when exposed to chloride environment. Such surfaces that require frequent reapplication and are subject to damage by flaking or removal of the protective layer from the substrate, are protected using different methods such as painting, electroplating and few others. The cost of corrosion can be very high. Corroded components are either discarded or simply replaced, the downtime and safety hazards can be at a high cost to an industry. Corrosion control requires considerable knowledge of corrosion chemistry and of the system being evaluated^{3,4}.

The influence of reinforcements on the corrosion resistance of metal matrix composites is one of the major obstacles to the use of these coatings. Aluminium alloys based composite normally forms a protective oxide film against corrosion attack. The addition of a reinforcing phase could lead to further damage on the protective films, increasing the number

* Tshwane University of Technology, Pretoria, South Africa.

† Center for Scientific and Industrial Research—National Laser Centre, Pretoria, South Africa.

© The Southern African Institute of Mining and Metallurgy, 2011. SA ISSN 0038-223X/3.00 + 0.00. Paper received Dec. 2010; revised paper received Mar. 2011.

Microstructure and corrosion properties of Al(Ni/TiB₂)

of sites where corrosion can be initiated. Corrosion attacks are commonly initiated at the flaws or heterogeneities in the protective films due to the presence of intermetallic/ceramic particulates and intermetallic precipitates in the MMCs. Corrosion attacks are known to occur preferentially in and around reinforcing particles or reinforcement-matrix interface. Corrosion of aluminium MMCs have been studied by different researchers but the information available in the open literature on corrosion of Al-based composite is sometimes contradictory. There are different Al alloy matrices available and also different metals/alloys/ceramics that can be used as reinforcement materials which often exhibit different corrosion behaviour. Laser processing parameters influence to a large extent the microstructure evolved and consequently the corrosion behaviour of the coatings so produced³⁻⁵.

Majumdar *et al.* developed a hard *in situ* titanium boride-dispersed Al matrix composite layer on Al substrate and evaluated the pitting corrosion property of laser composite in 3.56 per cent NaCl solution and compared it with that of as-received Al. The authors stated that the corrosion resistance was marginally deteriorated due to the presence of TiB₂ and TiB particles in the matrix². Yue *et al.* carried out laser surface treatment of 7075 alloy which produced two aluminium oxide layers at the surface of the laser-melted zone. From the potentiodynamic polarization results, the corrosion current was reduced by as much as six times and a passive region was obtained. The untreated specimen suffered widespread pitting corrosion, whereas the laser-treated specimen came under isolated attacks³. Chiu *et al.* modified the surface of AISI 316L stainless steel with NiTi using a laser surface alloying method. The results showed that the corrosion resistance of the laser alloyed sample is slightly inferior to that of the AISI 316L substrate. This was attributed to the presence of defects and inhomogeneities arising from melting, solidification and overlapping tracks in laser processing⁵. Tjong and Huo worked on series of solutions containing different concentrations of cerium chloride and hydrogen peroxide at 30°C to form protective conversion films on *in situ* Al-based composite. The compact conversion film improved the corrosion resistance during exposure to NaCl solution⁴.

It is therefore the aim of the present study to synthesize intermetallic matrix composite coatings on AA1200. The effects of TiB₂/Ni reinforcements with varying weight ratios on the corrosion properties and microstructures of the resultant intermetallic matrix composite coatings are studied. The influence of laser surface alloying processing parameters on the quality of fabricated coatings will also be investigated.

Experimental

The starting materials in this study include powders of Ni and TiB₂. These powders were mixed in different ratios as 30 wt per cent TiB₂+70 wt per cent Ni; 40 wt per cent TiB₂+60 wt per cent Ni; 50 wt per cent TiB₂+50 wt per cent Ni. A Philips PW 1713 X-ray diffractometer fitted with a monochromatic Cu K α radiation set at 40 kV and 20 mA was used to determine the phase composition of powder. The scan was taken between 10° and 80° 2 theta (2 θ) with a step size of 0.02 degree. The powder particle morphology and size

distribution were analysed using a scanning electron microscope SEM and Malvern Mastersizer 2000 image analyser. Phase identification was done using Philips Analytical X'Pert HighScore® software with an in-built International Centre for Diffraction Data (ICSD) database.

The chemical composition of the substrate used in this experiment is given in Table I. A commercially pure form of AA1200 aluminium plate is chosen to be the substrate material. Al and its alloys have been chosen as the matrix material due to their low melting point, low density, wide liquid temperature range and good formability. AA1200 is cheap compared to other grades of aluminium and, as such, if the properties can be improved, it can be used as replacement for the other expensive grades of aluminium. Because nickel is known to be highly corrosion resistant in many environments the reinforcement proportion chosen ranges between 50 and 70% Ni; TiB₂ is a ceramic material that exhibits good oxidation resistance, hence it was chosen to have a lower proportion of 50% and below.

The substrate was cut and machined to dimensions 100 × 100 × 6 mm; then it was subjected to sand blasting to clean the surface and improve absorptivity of the laser beam. The powder combinations were taken one at a time and were fed into the molten pool by means of an argon gas stream. Laser surface alloying was then carried out using a high power Rofin Sinar Nd: YAG solid-state laser. The laser is delivered to the target material through fibre optics. A Kuka robot is used to move the alloying head. The laser parameters used are shown in Table II. Single tracks of Al-TiB₂-Ni laser alloyed samples were made on substrates. The scan speed was varied while the laser power was held constant. After careful checks during the optimization process, two samples were selected per reinforcement proportion (Table II).

Characterization of laser coatings

The cross-section of alloyed samples were cut and polished, and were etched with Keller's reagent. The microstructures of the new phases formed were characterized by optical and scanning electron microscopes. The characteristics of the phases were studied by means of x-ray diffraction.

Electrochemical tests

A linear potentiodynamic scan was used to carry out the electrochemical corrosion behaviour of the samples. Electrochemical measurements were done using an Autolab potentiostat (PGSTAT30 computer controlled) with the General Purpose Electrochemical Software (GPES) package version 4.9. All the measurements were made at room temperature using 3.65 per cent NaCl. The solution for the study was prepared from analytical grade reagents and distilled water.

Table I

Chemical composition of the substrate material

Element	Al	Fe	Cu	Si
Composition (wt.%)	Balance	0.59	0.12	0.13

Microstructure and corrosion properties of Al(Ni/TiB₂)

Table II

Laser parameters and composition used during the laser alloying experiments

Sample no.	System (Al- TiB ₂ -Ni) composition	Power (kW)	Beam diameter (mm)	Scan speed (m/min)	Powder feed rate (g/min)	Shielding gas	Shielding gas flow (ℓ/min)
17	30%TiB ₂ +70%Ni	4	3	0.6	2	Argon	4
19	30%TiB ₂ +70%Ni	4	3	1.0	2	Argon	4
23	50%TiB ₂ +50%Ni	4	3	0.6	2	Argon	4
25	50%TiB ₂ +50%Ni	4	3	1.0	2	Argon	4
27	40%TiB ₂ +60%Ni	4	3	0.6	2	Argon	4
30	40%TiB ₂ +60%Ni	4	3	1.0	2	Argon	4

Samples 17 and 19 (30 per cent TiB₂+70 per cent Ni); 23 and 25 (50 per cent TiB₂+50 per cent Ni); 27 and 30 (40 per cent TiB₂+60 per cent Ni) had a surface area of 0.14, 0.13, 0.13, 0.13, 0.18 and 0.13 cm² respectively. An electrochemical cell consisted of working electrode (samples) graphite rods as the counter electrodes and a silver/silver chloride 3 M KCl electrode as the reference electrode (SCE). The specimens were mounted in epoxy resin, and ground down to 1200 grit silicon carbide paper prior to the measurements. The corrosion potential (E_{corr}), and corrosion rate were determined accordingly. The specimens were scanned from a potential of -1.5 V with respect to stabilized open circuit potential (E_{ocp}) at a rate of 0.25 mV s⁻¹. All the potentials reported were versus the SCE potentials.

Results and discussion

Characterization of starting materials

Particle size of powder

The particle size analysis of the starting powders was determined using the Malvern Mastersizer 2000 particle size analyser. Table III shows the summary of the particle sizes of the starting powders. The results from the table show that nickel has the highest average particle size, whereas the 50:50 admix powder of TiB₂ and Ni has the lowest average particle size. It was also observed that only the nickel powder showed average particle size greater than 30 μm.

Phase analysis of powders

Typical XRD spectrum of the mixtures can be seen from Figure 1. It was also observed that the intensity of the powders increased as the percentage of TiB₂ in the mixtures increased. The powders used were pure.

Electrochemical tests results

Comparative corrosion behaviour of the different weight percentages of TiB₂/Ni was studied in 3.65 per cent NaCl solution at room temperature. The corrosion data obtained from the electrochemical tests are reported accordingly. The effect of various Ni and TiB₂ contents on the corrosion behaviour of the alloys formed was investigated in the chloride solution. The results of measurements made for the specimens investigated are summarized in Table IV. Figure 2 shows the polarization curves of pure Al and all coatings immersed in aerated 3.65 per cent NaCl solution at 25°C. The

intersection of the cathodic and anodic Tafel plots gave the values of the corrosion current density (I_{corr}) and corrosion potential (E_{corr}). An investigation on the reactivity of the alloys, i.e. their susceptibility to corrode in the 3.65 per cent NaCl environment with time, was carried out using open circuit potential (OCP) measurements. The variations in the OCP values of the coatings were studied at zero applied current immediately after the immersion of the alloys in the different media for one hour. The variation in open-circuit potential as a function of time for all coatings and pure aluminium tested in 3.65 per cent NaCl, are presented in Figure 3.

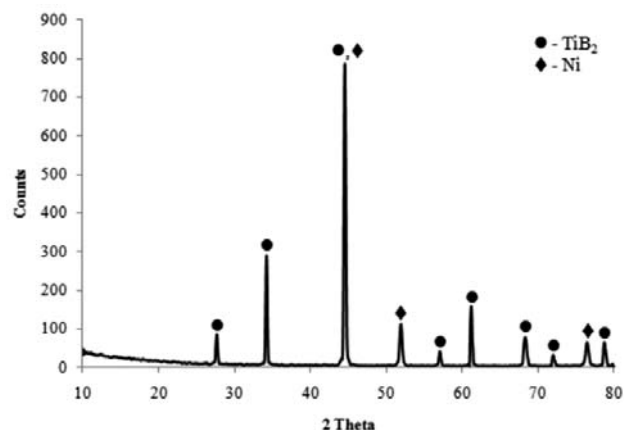


Figure 1—Typical XRD spectrum for the reinforcement powder mixture: 50%TiB₂+50%Ni

Table III

Particle size of the starting powders used in this work

Powder	D ₁₀ (μm)	D ₅₀ (μm)	D ₉₀ (μm)
Ni	49.954	68.535	93.991
TiB ₂	8.106	28.709	84.425
30%TiB ₂ +70%Ni	8.102	25.305	71.199
40%TiB ₂ +60%Ni	8.093	29.301	85.809
50%TiB ₂ +50%Ni	7.451	20.966	67.940

Microstructure and corrosion properties of Al(Ni/TiB₂)

Table IV

Summary of the potentiodynamic polarization results for all laser coatings

Sample label	E_{corr} (V)	I_{corr} (A/cm ²)	i_{corr} (A)	R_p (Ω)	β_a (V/dec)	β_c (V/dec)	Corrosion rate (mm/y)
Sample 17	-0.925	4.0×10^{-6}	5.6×10^{-7}	2.3×10^4	0.062	0.056	4.3×10^{-2}
Sample 19	-0.978	9.8×10^{-7}	1.3×10^{-7}	5.4×10^3	0.033	0.048	4.3×10^{-2}
Sample 23	-0.036	6.1×10^{-8}	7.8×10^{-9}	1.8×10^4	0.040	0.008	6.5×10^{-4}
Sample 25	-0.699	8.3×10^{-7}	1.2×10^{-7}	2.3×10^5	0.209	0.087	8.9×10^{-3}
Sample 27	-0.774	6.3×10^{-7}	1.1×10^{-7}	4.0×10^4	0.025	0.019	6.8×10^{-3}
Sample 30	-0.794	5.6×10^{-7}	7.3×10^{-8}	2.0×10^4	0.072	0.046	6.0×10^{-3}
AA1200	-1.036	2.3×10^{-6}	1.5×10^{-6}	2.6×10^3	0.072	0.128	3.7×10^{-2}

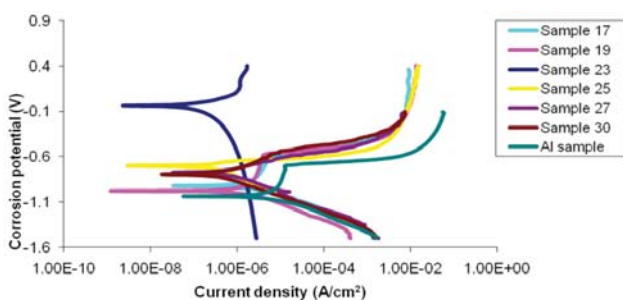


Figure 2—Potentiodynamic polarization curve for all laser coatings at 25°C

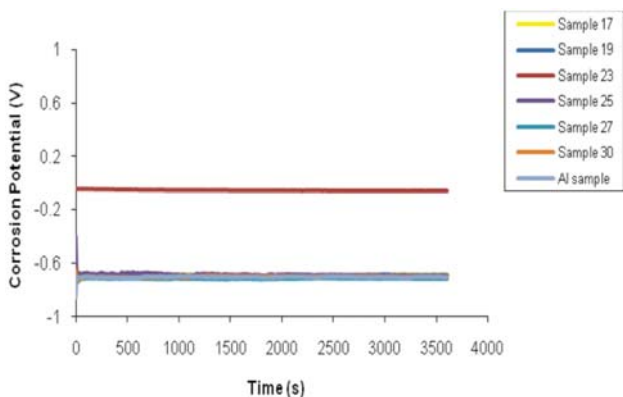


Figure 3—Open-circuit potential curve for all laser coatings

30 per cent TiB₂+70 per cent Ni coatings

From the XRD spectrum, phase compositions of these coatings have been identified. Figure 4 is a typical XRD spectrum for 30 per cent TiB₂+70 per cent Ni laser coatings. Four phases were identified in these micrographs, which are the dendritic phase (AlNi₃; Ni₄B₃; TiB/TiB₂ phase (grey lumps) and AlB₁₀ to be the generally displayed phases for coatings made with this mixture. According to Huo and Tjong, AlNi₃ phase is an intermetallic phase that possesses dendritic structure and it is characterized by a very high melting point, low density, high specific modulus, good oxidation resistance and high hardness; hence it is an excessively brittle phase¹⁵. In the same way, the nickel

borides are very hard compounds. The excessive brittleness of these phases is responsible for the cracking observed on this set of coatings (Figure 5c). However, an increase in TiB₂ content generally reduced the formation of these phases, as indicated on the EDS result, and consequently the excessive brittleness of coatings also decreased.

Figures 5a and 6a show the SEM micrographs of the 30 per cent TiB₂+70 per cent Ni coatings fabricated using different laser scan speed. The laser alloyed intermetallic matrix coatings of these samples are fully dense and uniform; good metallurgical bonding is evident between the substrate and reinforcement.

The laser coatings are composed of the initial phase of Al-Ni dendrites and eutectics of TiB₂/Al and TiB₂/Ni distributed on the initial phases. It can be seen that there are changes in the microstructure as the scan speed increases, there are refinements in microstructure as well as changes in grain sizes and morphologies. Moreover, the volume fraction of powder mixture injected during LSA increased as the scan speed increased. This is attributed to the wider melt pool which makes space for more powder intake; since the laser power and laser beam diameter were held constant during alloying, the cooling rate for all samples are not constant because of speed variation. The life and serviceability of components coated is determined to a large extent by the depth of the composite layers.

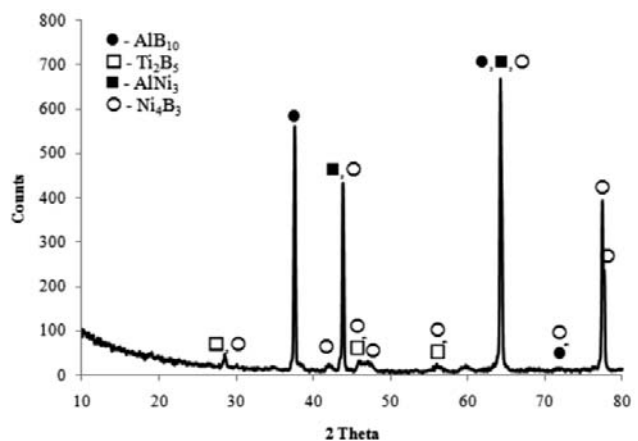


Figure 4—Typical XRD spectrum for the 30%TiB₂+70%Ni coatings

Microstructure and corrosion properties of Al(Ni/TiB₂)

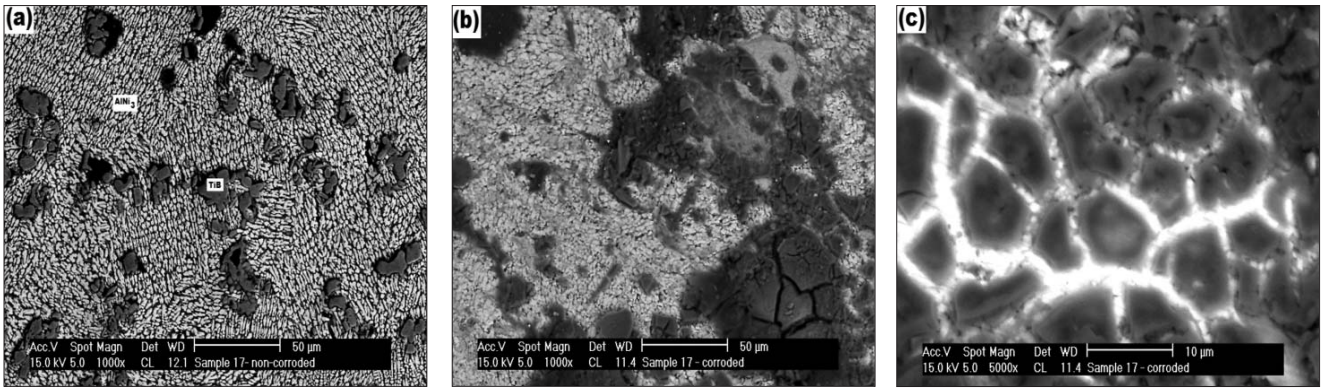


Figure 5—Scanning electron micrographs of sample 17 (a) before the corrosion test (b) after corrosion test (c) after corrosion test

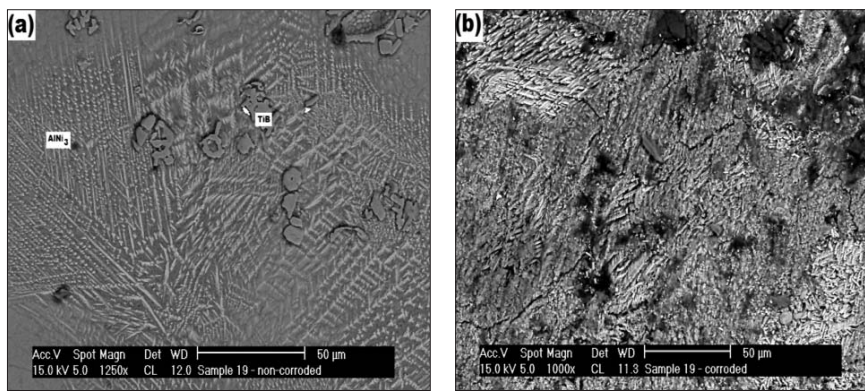


Figure 6—Scanning electron micrographs of sample 19 (a) before the corrosion test (b) after corrosion test

Figure 7 graphically represents the potentiodynamic curves and the OCP respectively for the 30 per cent TiB₂+70 per cent Ni coatings and that of pure Al. Table IV shows the results for all samples in the tested chloride solution. The curve for pure Al revealed a well defined corrosion potential E_{corr} followed by a passive region at the current densities around 2.3×10^{-6} Acm⁻². Figure 7 shows this set of coatings exhibit similar corrosion behaviour as pure Al.

All laser coatings fabricated with this reinforcement proportion exhibited a one order decrease in corrosion current compared to the pure Al, which is a good sign of a better corrosion resistance; however, if the values recorded for the corrosion current density are considered, all the alloyed samples and the untreated sample have corrosion current densities within the same range. All the coatings here displayed more anodic potentials, i.e. slightly higher E_{corr} . This change is within the experimental scatter of ± 400 mA, which suggests that galvanic action arose because of the presence of reinforcement powders. Sample 17 (70 per cent Ni at 0.6 m/min scan speed) was observed to exhibit passivity behaviour. Samples 17 and 19 exhibited similar corrosion behaviour (E_{corr} within the same range for both samples) as seen on the polarization curve; these two samples have a slightly higher corrosion resistance than the pure Al; see Figures 5b and 6b. However, if the corrosion rate is considered from Table IV, these two samples have corrosion rates approximately the same as the untreated sample. This is because of the active interface resulting from

reaction between the matrix alloy and the reinforcement during processing. This deterioration in corrosion resistance of these samples can be attributed to the presence of AlB₁₀ phase in their microstructures; furthermore, sample 17 exhibited larger corrosion current density (4.0×10^{-6} A/cm²) because it contained larger amounts of AlB₁₀ phase than sample 19. The galvanic effect between Al and TiB₂ is negligible. But the galvanic effect between the AlB₁₀ phase and aluminium matrix controls the corrosion of these samples. Actually, the active aluminium present in the galvanic couple consisting of AlB₁₀/Al eutectic phase in these samples corrodes preferentially when exposed to chloride solution. These samples exhibited severe corrosion attack and are less corrosion resistant than the unreinforced

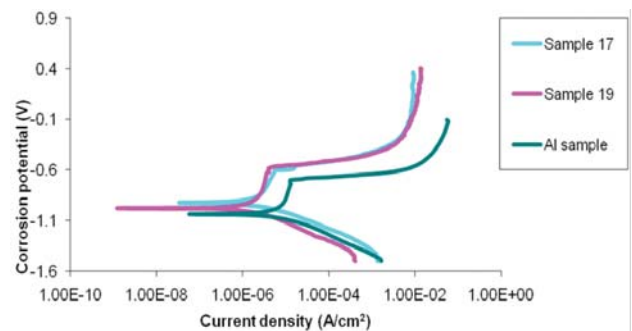


Figure 7—Potentiodynamic polarization curve 30%TiB₂+70%Ni coatings

Microstructure and corrosion properties of Al(Ni/TiB₂)

AA1200. The presence of different matrixes is a major contributor to galvanic corrosion and the decrease of corrosion resistance at interfacial areas, intergranular corrosion. The corrosion attack took place at the reinforcement-matrix interfaces as seen in Figure 5c for sample 17. According to Blanc and Guillaumin (quoted by Xu, Yue and Man), coarse intermetallic particles present in 6056 alloy were the major sources for the nucleation of pits, subsequently leading to intergranular cracking¹⁶. The accelerated corrosion at these sites is attributed to imperfect bonding and fissures in the intermetallic matrix composites and emphasizes the need for eliminating reactions between the Al and boron. Figures 5a and 6a shows the surface morphologies of samples 17 and 19. These samples are covered by the initial phase of Al-Ni dendrites which dominate the entire microstructure because of the high weight percentage of Ni. The protective films that are formed on the samples are illustrated in Figure 5c. It can be seen that this film just covered some local areas on the specimen surface. Local areas with high Ni content that are not protected by the film, severe cracks however, can be seen on the coatings.

50 per cent TiB₂+50 per cent Ni coatings

Figure 8 shows a typical XRD spectrum for 50 per cent TiB₂+50 per cent Ni laser coatings. The various phases identified in these coatings are Ni₄B₃, TiO_{0.997}, Ti, dendritic phase AlNi₃ and TiB/TiB₂ phase (grey). This set of coatings has phases identified in their spectrums similar to the coatings prepared by 30 per cent TiB₂+70 per cent Ni except for TiO_{0.997} phase.

All the coatings here displayed more anodic potentials, i.e. higher E_{corr} because of the phases in the Al matrix like the TiO_{0.997}, AlNi₃. These coatings are characterized by high peaks of TiO_{0.997}, which is probably the reason for their high corrosion resistances. They also have lower Ni content. All the coatings fabricated with 50 per cent TiB₂+50 per cent Ni powder mixture exhibited better corrosion resistance than pure aluminium. Samples 23 and 25 do not exhibit similar corrosion behaviour; their behaviours are completely different from each other and from pure Al, as shown in Figure 9. This can be attributed to the differences in their scan speeds during processing (Table II). These samples did not exhibit any passivation behaviour, although the passivation of pure Al was distinct. This can be attributed to heterogeneous surfaces because of the presence of different phases.

In the active corrosion stage, the corrosion current of laser alloyed samples are less than that of the untreated sample. From Table IV, a two orders magnitude decrease in corrosion current was achieved. According to electrochemical principles, the sample with lower corrosion current has a lower corrosion rate in active corrosion stage. The rate of corrosion for all laser coatings were decreased significantly by a two orders decrease in magnitude; it is obvious that sample 23 had the lowest corrosion rate as well as lowest corrosion current. As the passivation of the original sample occurs in the lower corrosion current compared with the laser treated sample, the passive tendency of the original sample is better than that of the laser coatings. It was concluded that the corrosion resistance of laser treated samples are better than that of pure Al.

The corrosion behaviour of sample 23 was unique amongst all the samples tested in this work (see Figure 2). Figure 10 shows the SEM micrographs of this sample before and after the corrosion test. At open circuit potential (E_{corr}), the corrosion current density (I_{corr}) of the untreated and laser-treated (sample 23) specimens are 2.3×10^{-6} A/cm² and 6.1×10^{-8} A/cm² respectively; a twofold decrease was achieved after alloying.

Sample 23 had the most positive corrosion potential, the least corrosion current density, and hence this sample exhibited the best corrosion resistance in the test solution compared to all samples tested. The incorporation of high proportion by weight of TiB₂ powder reinforcement into the matrix of the coatings generally does not lead to deterioration of the corrosion resistance. Monticelli *et al.* reported that the fine TiB₂ particles are beneficial in enhancing the pitting resistance of Al-based composite¹⁴. The 50 per cent TiB₂+50 per cent Ni coatings favour the formation of the protective films much more than the other reinforcement proportion. This is because of the higher content of Ti which promotes the formation of titanium oxide film. Ti element has the most positive corrosion potential despite its very negative thermodynamic potential for metal ion formation. The reason is that it forms a very protective oxide film at very negative potentials, and the film is resistant to breakdown by chloride ions. Monticelli *et al.* also indicated that a protective titanium oxide film can be formed on the surface of TiB₂ material when immersed in 3.5 wt.% NaCl solution at 25°C¹⁴.

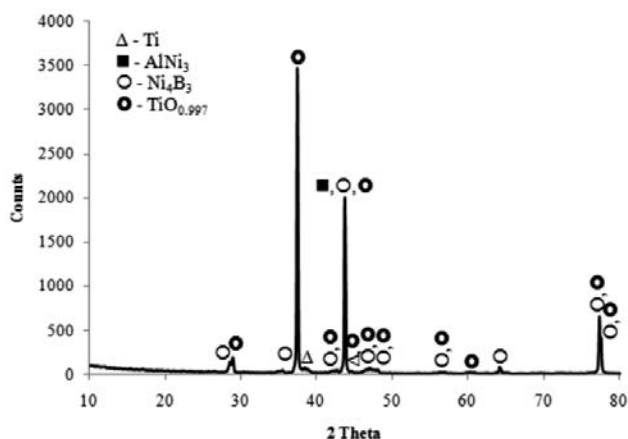


Figure 8—Typical XRD spectrum for the 50%TiB₂+50%Ni coatings

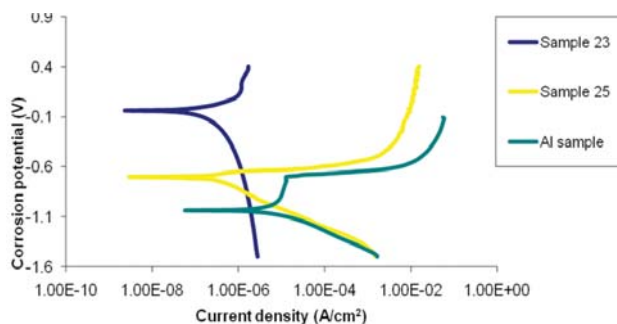


Figure 9—Potentiodynamic polarization curve 50%TiB₂+50%Ni coatings

Microstructure and corrosion properties of Al(Ni/TiB₂)

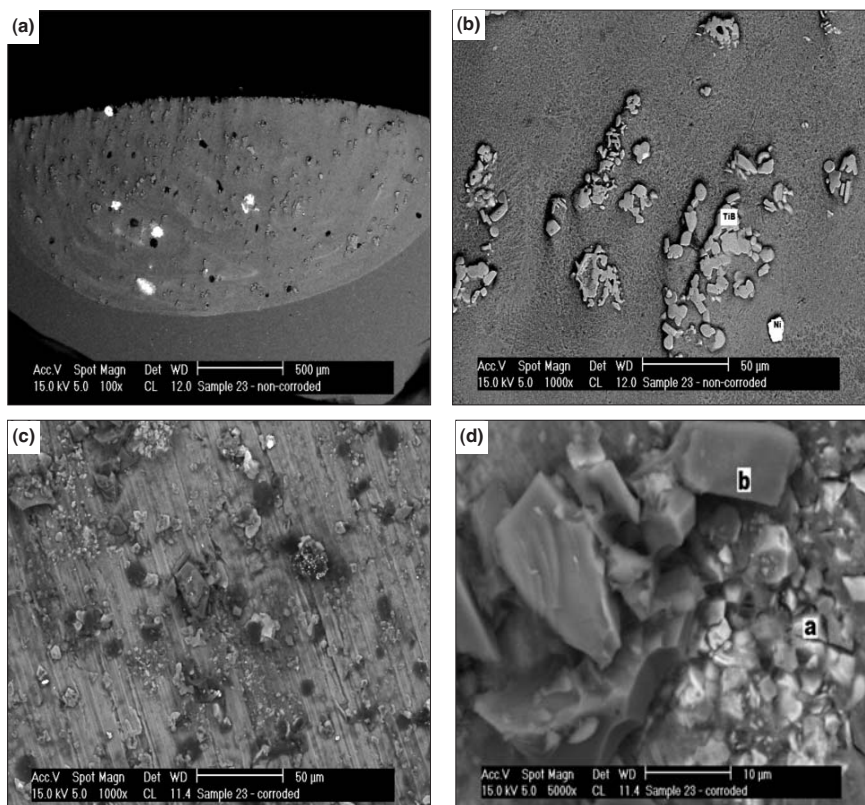


Figure 10—Scanning electron micrographs of sample 23 (a) overview of sample before the corrosion test (b) before corrosion test (c) after the corrosion test at low magnification (d) after the corrosion test at high magnification

Similarly, Al₂O₃ protective oxide film was also formed on these coatings when immersed in the chloride solution. However, these two oxides were seen to be present in the Al-matrix before the corrosion test as seen in the XRD spectrums (Figure 8). Therefore higher TiB₂ particle content contributes to higher corrosion resistance of samples 23 and 25. No formation of AlB₁₀ phase can be seen to be present in this set of coatings as evidenced by the x-ray spectrum. Figure 10d reveals two different areas on the protective oxide films: area a consists of high per cent of titanium oxide film while area b consists of high percent of Al₂O₃ film as indicated by energy dispersive spectrometry analysis (EDS). The protective films gave these samples a high corrosion resistance.

40 per cent TiB₂ + 60 per cent Ni coatings

Figure 11 is a typical XRD spectrum for 40 per cent TiB₂+60 per cent Ni laser coatings. From the XRD pattern, four phases were identified which are the dendritic phase AlNi₃, Ni₅TiO₇, Ni₃B, Al₂O₃.

At open circuit potential (E_{corr}), the results indicated that the corrosion current density (I_{corr}) of the untreated and laser-treated (sample 30) specimens are 2.3×10^{-6} A/cm² and 5.6×10^{-7} A/cm² respectively. This implies that a one order magnitude decrease in corrosion current density was obtained after the laser alloying treatment. This was considered to be due to the presence of the two dense oxide layers on top of the laser-alloyed zone. The two layers mainly consisted of TiO₂ and Al₂O₃. These are chemically stable

phases and serve as effective barrier to protect the matrix against corrosion attacks. The chloride ions tend to be very destructive because they prevent the formation of protective oxide films on the metal surface and thus increase the corrosion rate. Even a high quality alloy will corrode if its ability to form a passivating film is hindered. During polarization, slight passivation had occurred for samples 27 and 30; the region of passivation displayed for these samples is not as high as that of untreated sample. Typical surface morphologies of the laser coatings after the polarization test are shown in Figure 12. Apparently, the untreated specimen suffered from widespread pitting corrosion attacks but the

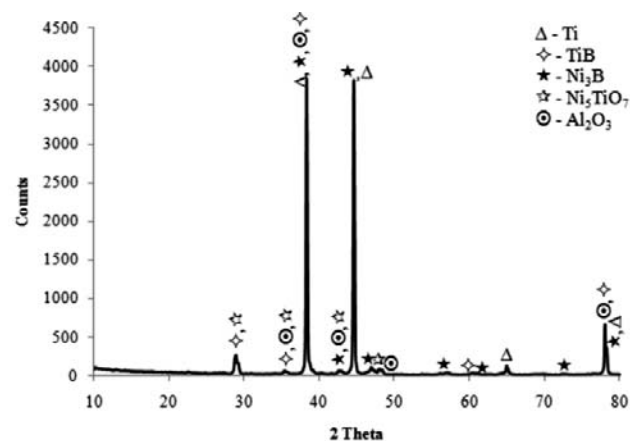


Figure 11—Typical XRD spectrum for the 40%TiB₂+60%Ni samples

Microstructure and corrosion properties of Al(Ni/TiB₂)

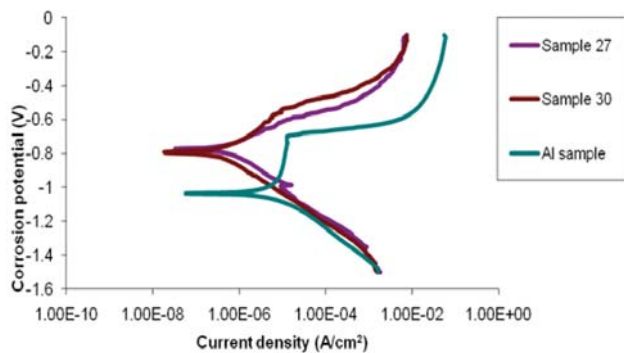


Figure 12—Potentiodynamic polarization curve 40%TiB₂+60%Ni samples

situation greatly improved after laser alloying. The attack in the laser coated specimens was difficult to see because the protective oxide layer, Al₂O₃ in form of a gelatinous mass, precipitated covering local regions on the surface and the TiO₂ coating covering some other regions. All samples exhibited better corrosion resistance than the pure Al. Also all the coatings have their corrosion potentials higher than that of pure Al. All the coatings here displayed more anodic potentials, i.e. higher E_{corr} because of the phases in the Al matrix like the Ni₅TiO₇, Al₂O₃, AlNi₃. These coatings possess peaks of Al₂O₃, this phase being corrosion resistant.

The corrosion current i_{corr} displayed for pure Al is 1.5×10^{-6} A and for sample 30 is 7.3×10^{-8} A; a two orders decrease in magnitude of the current was attained. From electrochemical theories, it is known that the corrosion rate is proportional to corrosion current density and that a reduction of the corrosion current density will enhance the passivity of the alloys. It can be seen that the laser coatings exhibit a reduction of both current density and active-zone-line slope when compared with the untreated sample. Similarly, a two order increase was also achieved in the polarization resistance (R_p) values of these samples. Comparing the corrosion rate of the samples, also a one order decrease in corrosion rate was observed. Therefore it can be inferred that all the coatings fabricated with 40 per cent TiB₂ + 60 per cent Ni powder mixture exhibited better corrosion resistance than pure aluminium, due to the formation of protective oxide films which delay stable pitting initiation. This set of coatings did exhibit slight passivation behaviour, although the passivation of pure Al was more distinct as seen in Figure 12. Similar results were observed when Man *et al.* alloyed NiCrSiB on Al6061, there was improvement in corrosion potential but the alloyed formed lacked passivation in 3.5% NaCl solution¹⁷.

OCP measurements for samples 27 and 30 indicated that there were breakdown in the films on their surfaces at the initial stages, followed by the formation of a new passive film after dissolution.

Corrosion current density, measured at the moment of electrode immersion in the solution, generally increases with increasing Ni content. The corrosion rate across board for the pure Al and laser coatings at 0.6 m/min are as follows:

Pure Al	3.7×10^{-2}
30 per cent TiB ₂ + 70 per cent Ni	4.3×10^{-2}
40 per cent TiB ₂ + 60 per cent Ni	6.8×10^{-3}
50 per cent TiB ₂ + 50 per cent Ni	6.5×10^{-4}

However, the result clearly shows an optimum amount of nickel is required before enhancement of corrosion resistance can be achieved. Clearly, a high nickel content does not improve corrosion resistance. This can be attributed to the microstructure of the coatings. XRD analysis of samples 17 and 19 shows high peaks of Al-B phase. The greatest factors that determine the formation of phases after alloying are the processing parameters. The properties of the coatings depend primarily on the microstructure that evolves during melting and cooling. At very low scan speeds the energy per unit mass increased significantly, resulting in the melting of Ni particles and subsequently a longer time in liquid state before being bonded and solidified, which in turn resulted in the formation of Al-Ni intermetallic as the initial phase on the matrix. The wider melt pool also led to a higher volume fraction of Ni being injected into the melt pool of the substrate and melted. The samples generally exhibited less negative corrosion potentials in all the tested solution as the TiB₂ proportion in the composites increased. The samples in general did not show any noticeable active-to-passive behaviour in the solution, but passivate spontaneously and go directly into a pseudo-passive state. One could observe a one order magnitude decrease in the corrosion rates for the samples as the TiB₂ increased.

A study on the reactivity of the samples, i.e. their tendencies to corrode in the 3.65 per cent NaCl environment with time, was carried out using open circuit potential (OCP) measurements. The variations in the OCP values of the alloys were studied at zero applied current immediately after the immersion of the alloys in the different media for one hour. The variation in open-circuit potential as a function of time for all the samples tested in 3.65 per cent NaCl is presented in Figures 3. The potential was observed to shift toward positive values for sample 23. The potentials of the samples generally confirmed the resistance of each of these samples as reported from the polarization report.

Stable passive films were formed on the surfaces of the samples after an initial increase in the potential, except samples 30 and 25 which indicated that there were breakdowns in the films on their surfaces at the initial stages, followed by the formation of a new passive film after dissolution. Sample 23 was observed to display the highest potential values, which confirmed why it exhibited the lowest corrosion rate in the potentiodynamic polarization test.

Conclusion

Multi-phase intermetallic matrix composite coatings have been successfully fabricated on Al substrate by laser surface alloying technique. The result of the investigation revealed that the surface quality and composition of phases changes with the weight proportion of the reinforcement powder and the laser processing parameters. Other results obtained include the following:

- ▶ Although the addition of nickel improved the corrosion resistance of the coatings, a high weight percentage of Ni does not necessarily lead to good corrosion

Microstructure and corrosion properties of Al(Ni/TiB₂)

resistance as would be expected. However, results showed that an increase in TiB₂ generally increases the corrosion resistances of coatings in this work.

- Coatings produced using the 30 wt per cent TiB₂+70 wt per cent Ni powder ratios exhibited the worst corrosion resistance, particularly sample 17 and 19. Deterioration of the corrosion resistance was attributed to the presence of AlB₁₀ phase. The process of degradation is accelerated by the AlB₁₀ and Al galvanic couple. Al-B compounds are strongly cathodic against metallic matrix and act as strong cathodic sites, facilitating dissolution of the protective coatings and enhancing corrosion attacks. Corrosion attack of the intermetallic matrix composites intensifies at very high concentration of the nickel particle and as the TiB₂ decreases.
- The 50 wt per cent TiB₂+50 wt per cent Ni coatings favour the formation of the protective films much more than the other coatings. This is because of the higher content of Ti which promotes the formation of titanium oxide film. Similarly, Al₂O₃ protective oxide film is also formed on these coatings when immersed in the chloride solution. The protective oxide films improved the corrosion resistance of coatings in NaCl solution. These were featured by the reduction in corrosion current and anodic current densities, and the displacement of corrosion potential to more positive values.
- The best corrosion resistance of the coatings was obtained at 50 wt per cent TiB₂+50 wt per cent Ni powder mixture and produced using the highest scan speed; this coating also exhibited the lowest microhardness value out of all the coatings tested.
- Finally, the corrosion potentials of all intermetallic matrix composite coatings were generally more noble than that of pure Al in chloride solution, resulting from the formation of protective surface films on reinforcing phases except for 30 wt per cent TiB₂+70 wt per cent Ni coatings, which exhibited behaviour close to that of pure Al.

References

1. NURMINEN, J., NAKKI, J., and VUORISTO, P. Microstructure and Properties of Hard and Wear Resistant MMC Coatings Deposited by Laser Cladding. *Int. Journal of Refractory Metals and Hard Materials*, vol. 27, 2009, pp. 472–478.
2. MAJUMDAR, J.D., CHANDRA, B.R., NATH, A.K., and MANNA, I. *In situ* Dispersion of Titanium Boride on Aluminium by Laser Composite Surfacing for Improved Wear Resistance. *Surface and Coatings Technology*, vol. 201, 2006, pp. 1236–1242.
3. YUE, T.M., YAN, L.J., CHAN, C.P., DONG, C.F., MAN, H.C., and PANG, G.K.H. Excimer Laser Surface Treatment of Aluminium Alloy AA7075 to Improve Corrosion Resistance. *Surface and Coatings Technology*, vol. 179, 2004, pp. 158–164.
4. TJONG, S.C. and HUO, H.W. Corrosion Protection of *in situ* Al-Based Composite by Cerium Conversion Treatment. *Journal of Materials Engineering and Performance*, vol. 18, 2009, pp. 88–94.
5. CHIU, K.Y., CHENG, F.T., and MAN, H.C. Corrosion Behaviour of AISI 316L Stainless Steel Surface-Modified with NiTi. *Surface and Coatings Technology*, vol. 200, 2006, pp. 6054–6061.
6. DU, B., ZOU, Z., WANG, X., and QU, S. *In situ* Synthesis of TiB₂/Fe composite coating by Laser Cladding. *Materials Letters*, vol. 62, 2008, pp. 689–691.
7. MAN, H.C., YANG, Y.Q., and LEE, W.B. Laser induced reaction synthesis of TiC+WC reinforced metal matrix composites coatings on Al 6061. *Surface and Coatings Technology*, vol. 185, 2004, pp. 74–80.
8. MAN, H.C., ZHANG, S., and CHENG, F.T. Improving the Wear resistance of AA 6061 by Laser Surface Alloying with NiTi. *Materials Letters*, vol. 61, 2007, pp. 4058–4061.
9. VAZIRI, S.A., SHAHVERDI, H.R., TORKAMANY, M.J., and SHABESTARI, S.G. Effect of Laser Parameters on Properties of Surface-Alloyed Al Substrate with Ni. *Optics and Lasers in Engineering*, vol. 47, 2009, pp. 971–975.
10. CHEN, S.P., MENG, Q.S., LIU, W., and MUNIR, Z.A. Titanium Diboride-Nickel Graded Materials Prepared by Field-Activated, Pressure-Assisted Synthesis Process. *Journal of Materials Science*, vol. 44, 2009, pp. 1121–1126.
11. XU, J. and LIU, W. Wear Characteristic of *in situ* Synthetic TiB₂ Particulate-Reinforced Al Matrix Composite formed by Laser Cladding. *Wear* 260, 2006, pp. 486–492.
12. BABU, S.S., KELLY, S.M., MURUGANANTH, M., and MARTUKANITZ, R.P. Reactive Gas Shielding during Laser Surface Alloying for Production of Hard Coatings. *Surface and Coatings Technology*, vol. 200, 2006, pp. 2663–2671.
13. CHEN, Y. and WANG, H.M. High-Temperature Wear Resistance of a Laser Clad TiC Reinforced FeAl *in situ* Composite Coating. *Surface and Coating Technology*, vol. 179, 2004, pp. 252–256.
14. MONTICELLI, C., FRIGNANI, A., BELLOSI, A., BRUNORO, G., and TRABANELLI, G. The Corrosion Behaviour of Titanium Diboride in Neutral Chloride Solution. *Corrosion Science*, vol. 43, 2001, pp. 979–992.
15. HUO, H. and TJONG, S.C. Corrosion Behaviour of Al-based Composites Containing *in situ* TiB₂, Al₂O₃ and Al₃Ti Reinforcements in Aerated 3.5% Sodium Chloride Solution. *Advanced Engineering Materials*, vol. 9, no. 7, 2007, pp. 588–593.
16. XU, W.L., YUE, T.M., and MAN, H.C. Nd:YAG Laser Surface Melting of Aluminium Alloy 6013 for Improving Pitting Corrosion Fatigue Resistance. *Journal of Materials Science*, vol. 43, 2008, pp. 942–951.
17. MAN, H.C., ZHANG, S., YUE, T.M., and CHENG, F.T. Laser Surface Alloying of NiCrSiB on Al6061 aluminium alloy. *Surface and Coatings Technology*, vol. 148, 2001, pp. 136–142. ◆